Proceedings of the INMM & ESARDA Joint Virtual Annual Meeting

August 23-26 & August 30-September 1, 2021

THE EFFECT OF SOURCE FUNCTION TYPES ON THE MASS FLOW AND ISOTOPIC DISTRIBUTION INSIDE A GAS CENTRIFUGE

Wisher Paudel
Houston Wood
Department of Mechanical & Aerospace Engineering
University of Virginia
Charlottesville, VA 22903, USA

ABSTRACT

The gas flow models inside a centrifuge domain are derived using the sources and sinks of mass, momentum, and energy. The system of equations governing the flow is combined to give non-homogeneous form of Onsager's equation without the pancake approximation, which is solved using finite element analysis. The derivations and details of the solution technique have been explored thoroughly in literature. This article focuses on the analysis of source distribution and strength for feed injection and the tails and product withdrawal via boundaries. Four different types of shape functions for the axial spreading of the sources and sinks are evaluated and their impacts on the flow and isotopic distributions are compared. The mathematical description of the source terms can be given as $S(x,y) = S_0 G(x) H(y)$, where S_0 is the strength, $H(y)$ is the axial distribution and $G(x)$ is the radial distribution. In the radial direction, the source distribution is assumed to be given by a delta function while in the axial direction, the four different cases considered include triangular, linear step, gaussian, and delta functions. The triangle and the gaussian are anticipated to be more realistic representation of the flow shapes and provide smoother distributions. In order to facilitate the comparison of these four functions, mass flow and concentration gradient plots are generated for an example hypothetical centrifuge.

INTRODUCTION

The purpose of the gas centrifuge is to produce uranium enriched in the fissionable isotope ^{235}U to be used as fuel in nuclear power reactors. The isotope separation in the centrifuge volume is influenced by the radial pressure gradient that forces the heavier ^{238}U molecules to be concentrated near the rotor wall and the lighter ^{235}U to be concentrated near the rotational axis. This radial separation can be greatly enhanced by establishing a countercurrent flow in the axial direction.

The fluid motions within a gas centrifuge are defined using Onsager's equation derived from the continuity, momentum, energy, and state equations for a viscous compressible gas. Onsager's equation assumes that the flow is a small perturbation from isothermal solid body rotation, which allows the linearization of the governing fluid equations [1]. It also assumes that for high rotation rates, all the gas is confined to a narrow annulus near the rotor wall. This relaxes the effects of cylinder curvature on the fluid dynamics of rapidly rotating gas. A numerical model of the flow with the inclusion of the curvature terms has been developed in literature [2].

An axial countercurrent circulatory motion of the gas flow is established and maintained by several disturbing mechanisms. These phenomena include temperature gradients on the rotor wall,

the injection of feed material, and the presence of stationary scoops for mass removal. The flow drives can be modeled as sources and sinks of mass, momentum, and energy [3].

There exist numerous flow studies for a centrifuge domain that make use of the sources and sinks [3] [4] [5]. In this work, we have focused on the definitions of the functions used to model these sources and sinks. We have removed the geometry of source distribution and have used simplified distribution functions [3]. While different authors have used different types of these distribution functions to model the sources, there is not a study in literature that evaluates the effects of such functions on the fluid flow and in turn isotope separation. Since the previous authors have not outlined their reasoning for selecting a particular function type in their analysis, this work seems essential in understanding the effects of each on the derived mass flow and diffusion solutions. Therefore, we will be using four different types of shape functions to simulate the radial and axial spreading of sources and sinks and compare their impacts and determine the most ideal shape. These four functions include the triangle, linear, gaussian, and Dirac delta functions. For a more quantitative comparison, the normalized root-mean square difference of the stream function and concentration gradients for each type will be evaluated and analyzed.

METHODOLOGY

The fluid dynamics model used in this study is Onsager's pancake as well as Onsager-Maslen with curvature effects with the inclusion of internal source/sink terms. The system of equations governing the flow combined to give the non-homogeneous form of Onsager's pancake equation is as follows:

$$(\boldsymbol{e^x}(\boldsymbol{e^x X_{xx}})_{xx})_{xx} + \boldsymbol{B^2 X_{yy}} = \boldsymbol{F(x,y)}, \qquad \textbf{(1)}$$

Where

$$\boldsymbol{F(x,y)} = \frac{\boldsymbol{B^2A^2}}{\boldsymbol{2ReS}}\int_x^\infty \left(\boldsymbol{\mathcal{J}_y - 2\mathcal{V}_y}\right)\boldsymbol{dx'} - \frac{\boldsymbol{B^2}}{\boldsymbol{4A^4}}\int_x^\infty \int_0^{x'} (\mathbf{M}_y \boldsymbol{dx"dx'} - \frac{\boldsymbol{B^2A^2}}{\boldsymbol{2ReS}}\left[\left(\boldsymbol{e^x \mathcal{U}_y}\right)_x + (\boldsymbol{e^x \mathcal{W}})_{xx}\right] \qquad \textbf{(2)}$$

And

$B = \frac{ReS^{\frac{1}{2}}}{4A^6}, S = 1 + \frac{PrA^2(\gamma-1)}{2\gamma}, where\ \gamma\ is\ the\ ratio\ of\ specific\ heats$

$A^2 = \frac{\Omega^2 a^2}{2RT_0}, where\ T_0\ is\ the\ average\ temperature\ of\ the\ gas\ and\ R\ is\ the\ specific\ gas\ constant$

$Re = \frac{\rho_w \Omega a^2}{\mu}, where\ \rho_w\ is\ the\ density\ at\ the\ wall, \Omega\ is\ the\ frequency\ of\ rotation$

$Pr = \frac{C_p \mu}{k}\ is\ the\ Prandtl\ number\ and\ C_p is\ the\ specific\ heat\ at\ constant\ pressure,$

$\mu\ is\ the\ viscosity\ of\ the\ gas, and\ k\ is\ its\ thermal\ conductivity$

The function X is a master potential whose derivatives yield the physical variables $u, v, w, \rho, and\ T$. The variables in Equation (2) M, $\mathcal{U}$, $\mathcal{V}$, $\mathcal{W}$, and $\mathcal{J}$ are sources/sinks of mass, radial momentum, angular momentum, axial momentum, and energy respectively. These terms are used to account for the presence of a scoop and the addition and withdrawal of gas. The solution of Equation (1)

provides the countercurrent flow inside the centrifuge. The non-homogeneous equation has been solved using finite difference methods [6] and finite-element methods [7] [8] [9] [4] [5].

The finite element solution for mass flow derived by Witt [4] and enhanced by Thomas [5] is used in this study to test the effects of various source types. The strength and distribution of these sources can be approximated by the feed entry and the tails-withdrawal scoop by separate analyses. The same simplifying assumptions regarding an idealized model of the feed interacting with the rotating gas utilized in [3] are used here as well. These assumptions include the fact that the gas enters the centrifuge rotor in an angularly symmetric process, the feed gas collides with the rotating gas and becomes indistinguishable after one collision, and the gas enters a vacuum as it exits the hole in the feed pipe and spreads in the axial direction before colliding with the rotating gas. The shape function for such axial spreading is the matter of analysis in this work. The sources terms can be generalized mathematically as

$$\boldsymbol{S(x,y) = S_0 G(x) H(y),} \tag{3}$$

where S_0 is the strength, $H(y)$ is the axial distribution and $G(x)$ is the radial distribution. These functions are then used as approximations of the mass, momentum, and energy terms in the right-hand side of Equation (1) to resolve the non-homogeneity of Equation (2).

Source Derivations

In the radial direction, the distribution is modelled by the Dirac delta function chosen because of its convenient mathematical analysis. Therefore, in Equation (3),

$$\boldsymbol{G(x) = \delta(x - x^*),} \tag{4}$$

where x^* is the radial location of the source and x is defined in scale heights. For the axial distribution, the four different functions mentioned previously will be used to derive the finite element solution to Equation (1). This derivation is based on what is reported in [4] and will not be repeated here. However, the analytical integrations for each source in the finite element calculations are included below.

Triangular Source

The description of the triangular shape of the distribution function is taken from Wood & Sanders [3]. The axial source distribution in Equation (34) is given by

$$\boldsymbol{H(y)} = \begin{cases} \boldsymbol{0} & (\boldsymbol{|y - y^*| > 0.5}) \\ \boldsymbol{-4|y - y^*| + 2} & (\boldsymbol{|y - y^*| \leq 0.5})\text{'} \end{cases} \tag{5}$$

where y^* is the axial location of the source and y is defined as the length divided by the rotor radius, i.e. $y = z/a$. $H(y)$ is a triangle of unit base with an altitude of 2. This function becomes a concentrated source for a centrifuge with larger aspect ratio as will be considered for this study.

In order to apply the above source function to the finite element solution of Equation (1), the right-hand side vector in Equation (5.65) from [4] needs to be modified. The matrix equation is:

$$\boldsymbol{[A]\vec{C} = \vec{D}}\text{, where } \boldsymbol{A_{k,k^*} = I_1 + I_2 + I_3} \text{ and } \boldsymbol{D_{k^*} = I_4 + I_5 + I_6 + I_7 + I_8} \tag{6}$$

Here, $k = 1,2,3 \ldots . K \; and \; k^* = 1,2,3, \ldots K, \; K = (M-1) * (N-1)$, where
$M = \#\; grid\; points\; in\; the\; radial\; direction, N = \#\; grid\; points\; in\; the\; axial\; direction.$

The eight integrals that make up Equation (6) have been derived and solved for by Witt. We focus on I_4 in this work, which accounts for the effects of sources and sinks in the mass flow. From Witt, Equation (5.74) is given by

$$\boldsymbol{I_4 = -\int_0^{x_T}\int_0^1 \phi_{k^*}\bar{S}\, dy\, dx\text{, where}} \tag{7}$$

$\phi_k(x,y) = \sigma_i(x)\lambda_j(y)$ is the product of the finite element shape functions given by σ in the radial direction and λ in the axial direction.

$$\boldsymbol{\bar{S} = -\frac{Re^2}{64A^{16}Z^2} * \frac{1+\hat{k}\eta^2}{\eta^4}\int_x^{x_T}\int_0^{x'}\frac{\partial S_M}{\partial y}\, dx"dx'} \tag{8}$$

Equation (85) is given here only for the mass source. Our four different source functions will solely evaluate the mass distribution at the feed. The momentum exerted by the scoop and mass sinks at the exits will be kept consistent with the analysis performed by Witt. Additionally, to simplify the derivations, the feed is modelled as a source of mass and scoop as a sink of angular momentum.

From Equation (8), the derivative term, $\frac{\partial S_M}{\partial y}$, for the triangular function defined in Equation (5) is obtained as:

$$\boldsymbol{\frac{\partial S_M}{\partial y} = S_0 * \delta(x - x^*) * \frac{\partial H}{\partial y}} \tag{9}$$

$$\boldsymbol{\frac{\partial H}{\partial y} = \begin{cases} 0 & (|y - y^*| > 0.5) \\ -\frac{4y-2}{|y-y^*|} & (|y - y^*| \le 0.5) \end{cases}} \tag{10}$$

Plugging Equation (9) into Equation (8),

$$\boldsymbol{\bar{S} = -\frac{Re^2}{64*A^{16}*Z^2} * \frac{1+\hat{K}\eta^2}{\eta^4} * S_0 * \frac{\partial H}{\partial y} * \left(\int_x^{x_T}\int_0^{x'}\delta(x' - x^*)\, dx''\, dx'\right)} \tag{11}$$

The double integral in Equation (11) can be simplified further down to:

$$\boldsymbol{\bar{S} = -\frac{Re^2}{64*A^{16}*Z^2} * \frac{1+\hat{K}\eta^2}{\eta^4} * S_0 * \frac{\partial H}{\partial y} * \left(\int_x^{x_T} x' * \delta(x' - x^*)\, dx'\right)} \tag{12}$$

Plugging Equation (12) into Equation (7) yields the expression for I_4.

$$\boldsymbol{I_4 = \frac{Re^2}{64A^{16}Z^2} * \frac{1+\hat{k}\eta^2}{\eta^4} * S_0 \int_0^{x_T}\sigma(x) * \left(\int_x^{x_T} x' * \delta(x' - x^*)\, dx'\right)dx * \int_{y^*-0.5}^{y^*+0.5} -\frac{4y-2}{|y-y^*|}\left(\lambda(y)\right)dy} \tag{13}$$

A new Matlab script is developed to solve Equation (13), which is then used as the right-hand side vector of the finite element problem given by Equation (1). The integrals in Equation (13) are evaluated numerically using the built in Matlab© solvers.

Linear Step Function Source

The axial distribution of the source of this type is defined by Wood [10] as follows:

$$H(y) = \begin{cases} 0 & 0 \le y < y^* - 1.5 \\ y & y^* - 1.5 \le y \le y^* + 1.5 \\ 0 & y^* + 1.5 < y \le y_T \end{cases} \quad (14)$$

Equation (14) is a slightly modified version of the same expression defined in [10] where a constant value of $H(y)$ is replaced with a variable, y, in and around the axial location of source. This change was necessary to ensure that the y derivative of H exists as required by Equation (9). Thus, following the same derivation as for the triangular source above, the expression for I_4 can be evaluated as:

$$\frac{\partial H}{\partial y} = \begin{cases} 0 & 0 \le y < y^* - 1.5 \\ 1 & y^* - 1.5 \le y \le y^* + 1.5 \\ 0 & y^* + 1.5 < y \le y_T \end{cases} \quad (15)$$

Plugging $\frac{\partial H}{\partial y}$ into Equation (9) and the resulting expression for $\bar{S}$ into Equation (7) yields:

$$I_4 = \frac{Re^2}{64A^{16}Z^2} * \frac{1+\hat{k}\eta^2}{\eta^4} * S_0 \int_0^{x_T} \sigma(x) * \left(\int_x^{x_T} x' * \delta(x' - x^*)\, dx'\right) dx * \int_{y^*-1.5}^{y^*+1.5} 1 * (\lambda(y)) dy \quad (16)$$

Gaussian Distribution Source

The expression for the gaussian source is taken from Gunzburger, Wood, and Jordan [8].

$$S_M = S_0 \delta(x - x^*) * e^{-\alpha * (y - y^*)^2} \quad (17)$$

A value of α was chosen such that $S_M = 10^{-6} * S_0$ at $(x - x^*)^2 + (y - y^*)^2 = 1$. Thus,

$$S_M = 10^{-6} S_0 = S_0 * e^{-\alpha * 1} \grave{a}\ \alpha = -ln(10^{-6}) \quad (18)$$

$$\frac{\partial S_M}{\partial y} = S_0 \delta(x - x^*) * -2\alpha(y - y^*) e^{-\alpha((y-y^*))^2} \quad (19)$$

$$\bar{S} = -\frac{Re^2}{64 * A^{16} * Z^2} * \frac{1+\hat{K}\eta^2}{\eta^4} * \left(\int_x^{x_T} \int_0^{x'} \frac{\partial S_M}{\partial y} dx" dx'\right) \quad (20)$$

$$I_4 = \frac{Re^2}{64A^{16}Z^2} * \frac{1+\hat{k}\eta^2}{\eta^4} * S_0 \int_0^{x_T} \sigma(x) * \left(\int_x^{x_T} x' * \delta(x' - x^*)\, dx'\right) dx * \int_0^1 \lambda(y) * -2\alpha(y - y^*) e^{-\alpha * ((y-y^*))^2}\, dy \quad (21)$$

Delta Sources

The last model of the source distribution is produced using delta functions in both the radial and axial directions. This model is utilized by the finite element solution developed by Witt [4]. The derivations of the I_4 integral using the delta functions is obtained as follows:

$$S_M = S_0 \delta(x - x^*) \delta(y - y^*) \quad (22)$$

$$\frac{\partial S_M}{\partial y} = S_0 \delta(x - x^*) \delta'(y - y^*) \quad (23)$$

$$\bar{S} = -\frac{Re^2}{64 * A^{16} * Z^2} * \frac{1+\hat{K}\eta^2}{\eta^4} * S_0 * \delta'(y - y^*) * \left(\int_x^{x_T} \int_0^{x'} \delta(x" - x^*)\, dx" dx'\right) \quad (24)$$

$$\bar{S} = -\frac{Re^2}{64 * A^{16} * Z^2} * \frac{1+\hat{K}\eta^2}{\eta^4} * S_0 * \delta'(y - y^*) * \int_x^{x_T} He(x' - x^*) dx', \textit{ where } He \textit{= Heaviside function} \quad (25)$$

$$\overline{S} = -\frac{Re^2}{64*A^{16}*Z^2} * \frac{1+\hat{K}\eta^2}{\eta^4} * S_0 * \delta'(y-y^*) * \begin{cases} x_T - x^*, & x \le x^* \\ x_T - x, & x > x^* \end{cases} \quad (26)$$

Plugging Equation (26) into Equation (7) and simplifying the resulting expression yields

$$I_4 = \frac{Re^2}{64A^{16}Z^2} * \frac{1+\hat{k}\eta^2}{\eta^4} * S_0 * \left[x_T * \int_0^{x_T} \sigma(x)\, dx - x^* \int_0^{x^*} \sigma(x)\, dx - \int_{x^*}^{x_T} x * \sigma(x)\, dx\right] * \int_0^1 \lambda(y) * \delta'(y-y^*)\, dy \quad (27)$$

Using the properties of the delta function, the y-integral in Equation (27) can be simplified further as

$$I_4 = \frac{Re^2}{64A^{16}Z^2} * \frac{1+\hat{k}\eta^2}{\eta^4} * S_0 * \left[x_T * \int_0^{x_T} \sigma(x)\, dx - x^* \int_0^{x^*} \sigma(x)\, dx - \int_{x^*}^{x_T} x * \sigma(x)\, dx\right] * \lambda'(y^*) \quad (28)$$

Therefore, using Equations (28), (21), (16), and (13), new Matlab© scripts are developed for each to solve the finite element solution of the mass flow.

RESULTS

The effects of the source functions on the mass flow and isotopic diffusion are explored inside a hypothetical Rome centrifuge [11]. The physical and operating parameters for this machine can be found readily in literature and has been reiterated below.

Table 1: Machine parameters for the Rome centrifuge.

Parameter	Variable	Unit	Rome
Radius	a	m	0.25
Length	z_H	m	5
Average gas temperature	T	K	320
Wall pressure	p	$torr$	100
Cut	θ	$-$	0.5
Speed	v	$\frac{m}{s}$	600
Feed flow rate	F	$\frac{kgUF_6}{s}$	70
ΔT_{Wall}	-	K	6.92
Scoop drag	-	$Dynes$	1983

The values of the countercurrent flow drive parameters including the feed rate, end-to-end temperature difference at the rotor wall, and the drag force exerted by the stationary scoop on the rotating gas are taken from the ideal calculations performed in [5] for Rome machine spinning at 600 m/s. For the total flow drive solution, the feed entry is modelled as a source of mass, where each of the four different functions described above are used to simulate the spread of the mass source, and the scoop is modelled as a sink of angular momentum, which is represented as a point at the location of the scoop extraction hole using delta functions in both the radial and axial directions. The streamlines of the countercurrent flow and the corresponding concentration gradient for the $^{235}UF_6$ isotope obtained for each source are presented below. Natural uranium is used at the feed for the diffusion equation solved using finite element analysis as outlined by Paudel [12].

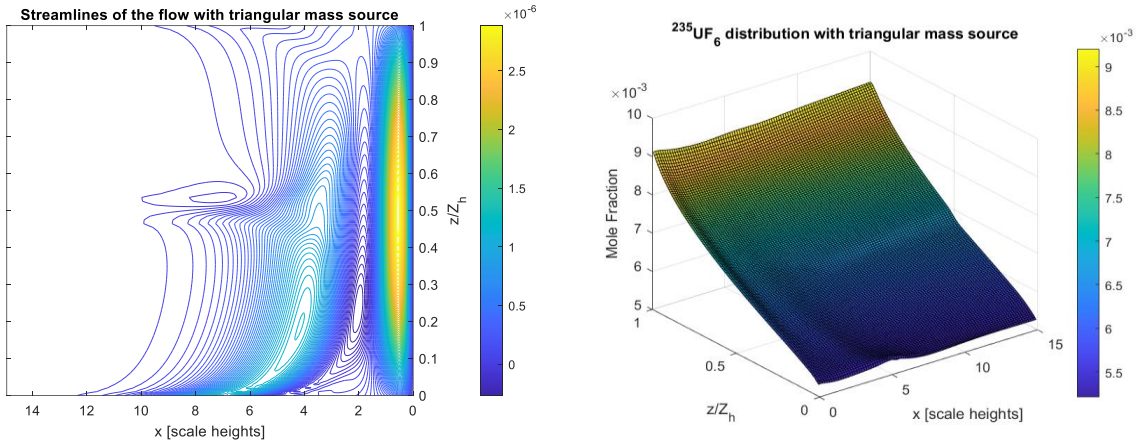

Figure 1: Streamlines of the total drive flow solution obtained using triangular mass source at the feed (left) and the corresponding ^{235}U concentration gradient (right)

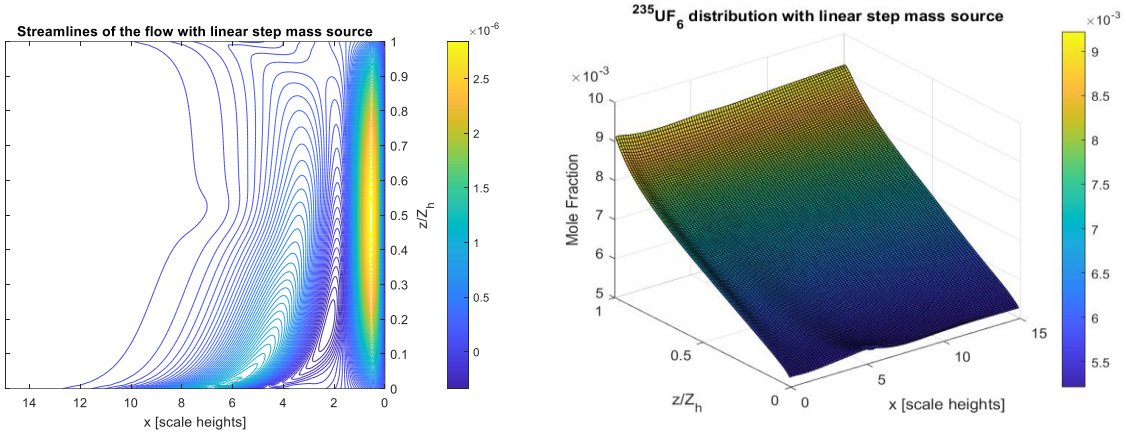

Figure 2: Streamlines of the total drive flow solution obtained using linear step mass source at the feed (left) and the corresponding ^{235}U concentration gradient (right)

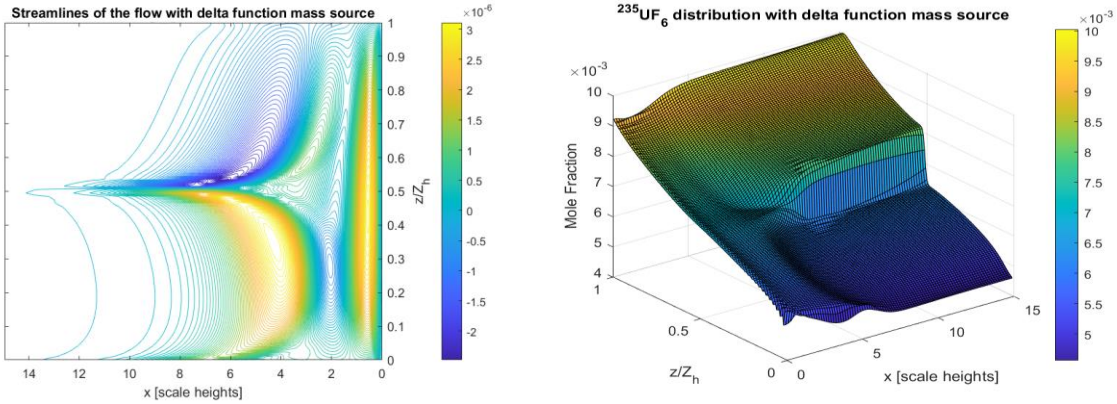

Figure 3: Streamlines of the total drive flow solution obtained using delta function mass source at the feed (left) and the corresponding ^{235}U concentration gradient (right)

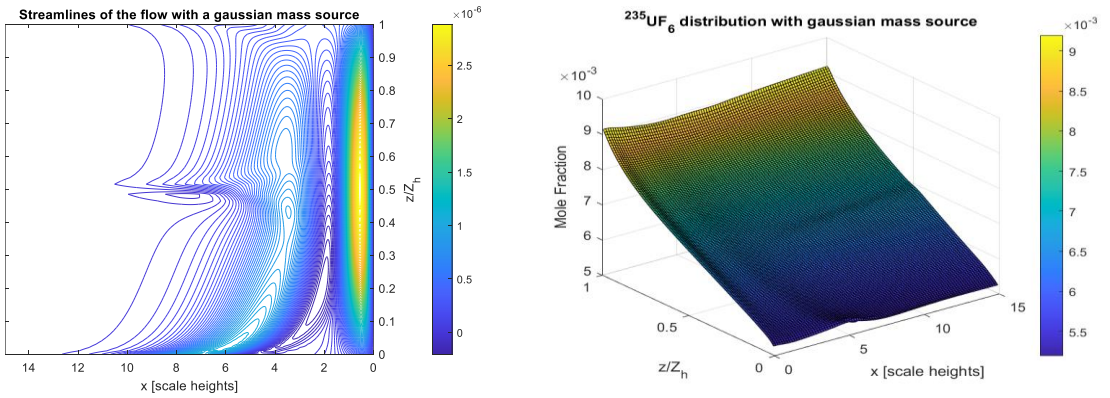

Figure 4: Streamlines of the total drive flow solution obtained using gaussian mass source at the feed (left) and the corresponding ^{235}U concentration gradient (right)

The streamlines of the mass flow solution using each of the four different source functions have been presented above on the left. The x-axis represents the non-dimensional radial direction of the centrifuge from x=0 at the wall to x=15 at the "top of the atmosphere." The y-axis is the axial dimension divided by the rotor height, Z_h, that goes from the bottom of the machine at y=0 to the top at y=1. It can be observed that much of the flow for each case is concentrated very near the rotor wall between x=0 and x=2. The color bar indicates the peaks and troughs of the countercurrent flow field with higher elevation corresponding to increasing magnitude shown on the right. For each source, the gas enters the centrifuge rotor at the axial midpoint and at roughly around x=12. The point where the feed interacts with the rotating gas can be visually observed in all the figures between x=7 and x=10.

The key distinction between the effects of the different functions on the countercurrent flow is on the severity of the separation of the upstream and downstream flows. The streamlines generated using the delta function in Figure 3 show the sharpest division of the flow at the axial midpoint between the two halves of the centrifuge. This result is expected based on the mathematical derivation applied using the delta function as highlighted in Equations (22)-(28). The source defined in Equation (22) has the Dirac delta function in both directions. While the discontinuous nature of the delta function is accounted for in the radial direction by smoothing its effects using integrations, it is elevated further in the axial direction by the derivative in Equation (23). To further understand the use of integrations and derivatives, it is essential to examine the non-homogeneous part of the Onsager's equation given by Equation (2). It can be seen that the radial dependence of the source functions for energy, J, angular momentum, V, and mass, M, are integrated once or twice, smoothing out discontinuities leading to better convergence. On the other hand, the radial, U, and axial, W, momentum sources have one or two derivatives requiring functions with continuous derivatives. In order to get a smoother numerical convergence, the source functions therefore need to have at least one derivative that is continuous. Because the mass source in Equation (2) is derived once in y and the Delta source has a discontinuous derivative in that direction, the mass flow plot in Figure 3 produces sharp gradient around the feed location. This discontinuity in flow is translated onto the diffusion equation via the axial mass flux term and results in the sharp gradient around the axial midpoint as seen in the concentration distribution plot on the right side of Figure 3. The use of other three source types with continuous derivatives reduces this nonphysical break in the concentration plots. Based on visual inspection of the flow streamlines and concentration surface plots, the linear step mass source function provides the smoothest solutions followed by the triangular source and the

gaussian. This can be explained by the fact that the finite element derivation of the flow equations makes use of the linear shape functions in the axial direction and thus the linear step source serves as the best fit to the approximation of the countercurrent flow. The gaussian source can be improved to provide the smoothest solution by selecting a smaller value of the decay constant, α, which would prevent the source from deteriorating at a rapid rate and resulting in accelerated change.

To better quantify the variability between the sources, the normalized root-mean-square (RMS) difference of the stream functions and the ^{235}U concentration gradients is calculated. The normalized RMS, d, is given by the following equation:

$$d = \left[\frac{\int_0^{y_T}\int_0^{x_T}(\psi_1-\psi_2)^2\,dx\,dy}{\int_0^{y_T}\int_0^{x_T}\psi_1^2\,dx\,dy}\right]^{\frac{1}{2}}, \qquad (29)$$

where ψ_1 is the stream function and/or concentration gradient matrix of source type 1 and ψ_2 is the corresponding matrix of source type 2.

Table 2: Normalized RMS of the stream function and concentration gradient between the sources

Source Types, (ψ_1 $vs.$ ψ_2)	d (Stream Function)	d (^{235}U Concentration Distribution)
Triangle vs. Gaussian	0.1686	0.0082
Triangle vs. Linear Step	0.2010	0.0077
Linear Step vs. Gaussian	0.2177	0.0050
Triangle vs. Delta	1.1775	0.0487
Gaussian vs. Delta	1.3688	0.0450
Linear Step vs. Delta	1.4217	0.0446

Table 2 quantifies the differences between each of the four sources and their effects on the flow and isotope diffusion. The delta function diverges the most from the rest of the sources as seen from Figure 3 and for the reasons discussed above. The normalized RMS values for the concentration distribution are a few orders of magnitude smaller than those for the stream functions, which indicates the effect of the sources is greater on the mass flow than on the isotopic concentrations. This is expected since the 2-D diffusion equation only includes the axial mass flux term from the mass flow solution. While the isotopic separation is partially influenced by the mass flux, it is also affected greatly by the molecular weight differences between the isotopes and the gas density gradient in the centrifuge rotor volume that are not influenced by the type of source functions used.

CONCLUSIONS

Four different mathematical functions were taken from literature and incorporated into the finite element solution for the mass flow inside a gas centrifuge to comprehend their effects on the source distribution. These source functions alter the streamlines of the flow as well as the isotopic concentration distribution with the greatest differences seen with the Dirac delta function. The discontinuity of the delta function needs to be lessened using smoothing techniques such as the one described in Wood and Sanders [3]. The other three sources provide relatively similar flow solutions. The impact on the concentration distribution is less than that on the mass flow since it is dictated not only by mass flux but also by the pressure and back diffusion of isotopes. The linear step function and the Gaussian distribution provide the smoothest countercurrent flow solutions and are anticipated

to be the best representation of the physics in the gas centrifuge. Future work can include the modification of the mass flow model that can accept any arbitrary function type with continuous derivatives of users' choosing to represent the sources and sinks of mass, momentum, and energy.

REFERENCES

[1] H. G. Wood and J. B. Morton, "Onsager's Pancake Approximation for the Fluid Dynamics of a Gas Centrifuge," *Journal of Fluid Mechanics,* vol. 101, no. 1, pp. 1-31, 1980.

[2] H. G. Wood,, J. A. Jordan and M. D. Gunzburger, "The Effects of Curvature on the Flow Field in Rapidly Rotating Gas Centrifuges," *J. Fluid Mech,* vol. 140, pp. 373-395, 1984.

[3] H. G. Wood and G. Sanders, "Rotating Compressible Flows with Internal Sources and Sinks," *Journal of Fluid Mechanics,* vol. 127, pp. 299-313, 1983.

[4] W. C. Witt, "The Onsager Equation with Curvature and Source Terms: A Finite Element Solution," University of Virginia, Charlottesville, VA, 2013.

[5] B. R. Thomas, W. C. Witt, W. Paudel and H. G. Wood, "A Finite Element Solution to the Generalized Onsager Model of Fluid Flow in a Countercurrent Gas Centrifuge," *Journal of Separation Science and Technology,* 2019.

[6] J. A. Viecelli, "Exponential Difference Operator Approximation for the Sixth Order Onsager Equation," *J. Comp. Phys.*, vol. 50, pp. 162-170, 1983.

[7] M. D. Gunzburger and H. G. Wood, "A Finite Element Method for the Onsager Pancake Equation," *Computer Methods in Applied Mechanics and Engineering,* vol. 31, no. 1, pp. 43-59, July 1982.

[8] M. D. Gunzburger, H. G. Wood and J. A. Jordan, "A Finite Element Method for Gas Centrifuge Flow Problems," *SIAM J. Sci. Stat. Comput.*, vol. 5, no. 1, pp. 78-94, March 1984.

[9] R. Bourn,, T. E. Peterson and H. G. Wood, "Solution of the Pancake Model for Flow in a Gas Centrifuge by Means of a Temperature Potential," *Comput. Methods Appl. Mech. Engrg.*, vol. 178, pp. 183-97, 1999.

[10] H. G. Wood, "Analysis of Feed Effects on a Single-Stage Gas Centrifuge Cascade," *Separation Science and Technology,* vol. 30, no. 13, pp. 2631-2657, 1995.

[11] "The Rome Machine, definition," in *Proceedings of the Fifth Workshop on Gases in Strong Rotation,* University of Virginia, Charlottesville, VA, June 1983.

[12] W. Paudel and H. Wood, "Two Dimensional Multi Isotope Separation in a Gas Centrifuge Using Finite Element Analysis," *Journal of Physics: Conference Series (In Progress),* 2021.